Desalination and Water Treatment
www.deswater.com
doi: 10.1080/19443994.2014.958110

56 (2015) 1929–1939
November

Taylor & Francis
Taylor & Francis Group

Adsorptive removal of acid red from aqueous solutions by cationic surfactant-modified bentonite clay

Manohar D. Mullassery[a,*], Noeline B. Fernandez[a], Thayyath S. Anirudhan[b]

[a]*Department of Chemistry, Fatima Mata National College, Kollam 691001, India, Tel. +91 9447110857; email: mdmullassery@gmail.com (M.D. Mullassery)*
[b]*Department of Chemistry, University of Kerala, Trivandrum 695581, India*

Received 26 May 2014; Accepted 6 August 2014

ABSTRACT

The performance of hexadecyltrimethylammonium chloride (HDTMA)-intercalated bentonite clay (organoclay) for the removal of acid red (AR) from aqueous solutions has been evaluated in this study. The adsorbent HDTMA-modified bentonite clay was prepared by the reaction of Na-bentonite with ($HDTMA^+$) cations equal to twice the cation exchange capacity of the Na-bentonite. The adsorbent characterization was done with the surface area analyzer, FTIR, SEM, XRD, TGA and potentiometric titrations. Maximum adsorption of AR onto organoclay has been found to be at pH 3.0. The Langmuir isotherm model was found to be the best fit model. The maximum adsorption capacity was found to be 140.84 μmol/g at 30˚C. Adsorption has been found to be endothermic and follows first-order reversible kinetics.

Keywords: Na-bentonite; Adsorption; Acid red; Isotherm; Desorption

1. Introduction

The presence of numerous dyestuffs with various chemical properties and adverse effects in surface and underground waterways has been a concern of the public and governments all around the world. Water-soluble anionic dyes like acid red (AR) and acid blue, which are one of the most important group of dyes used in textile dyeing industries, are used to dye fabrics like wool, nylon and silk. Total dye consumption worldwide was estimated to be more than 10^7 kg/year, and about 90% use is found in the textile industry. Consequently, approximately 1,000,000 kg/year of dyes are discharged into waste streams by the textile industry [1].

The discharge of dye-bearing wastewater into environment natural waterways from textile, paper, leather, tannery, plastics and cosmetics is the first contaminant that is recognized. Due to the colour and turbidity associated with dyes, they are highly visible and damage the aesthetic nature of the environment [2–4]. These dyes may also drastically affect photosynthetic phenomena in aquatic life due to reduced light penetration [5,6]. Many of these dye wastes are toxic and carcinogenic, and pose serious hazards to aquatic living organisms. As a result, the removal of colour from waste effluents has become environmentally important [7–9]. Dyes may also be problematic if they are broken down anaerobically in the sediment, as toxic amines are often produced due to the incomplete degradation by bacteria [10]. Direct discharge of dye-laden wastewater into municipal wastewater plants or

*Corresponding author.

the environment may cause the formation of toxic carcinogenic breakdown products. Today, more than 9,000 dyes are incorporated in a colour index, belonging to various chemical application classes. Water-soluble anionic group of dyes, one of the most important group of dyes used in textile dyeing industries, are used to dye fabrics like wool, nylon and silk.

Various techniques have been employed for the removal of dyes from wastewaters. The most widely used methods for removing color effluents from water include chemical precipitation, ion exchange, ozonation, solvent extraction, adsorption, membrane filtration, etc. [11]. Due to the low biodegradability of dyes, a conventional biological treatment process is not very effective. Adsorption has been found to be superior to other techniques for wastewater treatment in terms of low cost, simplicity of design, ease of operation and insensitivity to toxic substances [12,13]. Adsorption also appears to be most effective, especially for effluents with moderate and low concentrations. Several wastes and residues have been investigated for the adsorption of dyes with varying success [14–20]. Activated carbon adsorption is one of the recommended technologies for the removal of dyes from wastes. However, it is not widely used in practice due to low capacities of commercially available activated carbon. Therefore, a new and promising class of adsorbents is needed for alleviating the problems caused by textile dyes. Recently, adsorption due to clay has drawn much attraction due to its low cost, easy availability, and possibility of enhanced adsorbabilities by surface modification.

Bentonite is a natural clay mineral that is found in many places of the world. Any clay of volcanic origin that contains montmorillonite is referred to as bentonite. It has a 2:1 configuration consisting of two silicon–oxygen tetrahedral sheets and one aluminium–oxygen–hydroxyl octahedral sheet. The adsorptive properties of bentonite can be improved by surface modification. Replacement of inorganic exchange cations with quaternary amine cations $[(CH_3)_2NHR]^+$, where R is a large alkyl hydrocarbon chain, yields organoclays, with organophilic clay surfaces by simple ion-exchange resins. It is generally accepted that the adsorption of hydrophilic long chain quaternary ammonium cations onto clays occurs according to the ion exchange mechanism [21,22]. The extent of adsorption of such cations can approach two times the cation exchange capacity (CEC). The van der Waal's hydrophilic interactions are suggested to operate in such cases and lead to a bilayer of alkyl chains with positive charges exposed to the bulk of the solution [23]. Earlier workers [24–28] reported that the lyophilic tails from cations of long chain quaternary ammonium salts, previously retained on the clay, lead to the adsorption of organic compounds such as benzene, toluene, phenol and its chlorinated compound such as 2,4,6-trichlorophenol, and reactive blue and herbicides. In the present study, an attempt has been made to evaluate the removal of AR using hexadecyltrimethylammonium chloride (HDTMA)-intercalated bentonite clay.

2. Materials and methods

2.1. Materials

Bentonite clay, used for the preparation of organoclay, was procured from Sigma-Aldrich Chemie (Germany). Prior to its use, the bentonite clay was purified by sedimentation to obtain a particle size of < 100 μm. The clay was converted to Na^+-saturated form by washing it several times with 1.0 M NaCl and then with distilled water. The surfactant used for the present study, HDTMA with 99.0% purity, was purchased from Aldrich Chemicals (USA) and was used as supplied. AR was purchased from Sigma-Aldrich Chemie (Germany). The characteristics and chemical structure of AR is shown Table 1 and Fig. 1 respectively.

Table 1
Physical and chemical characteristics of AR 114 dye

Generic name	C. I. Acid Red 114
Color index number	23,635
Abbreviation	AR 114
Commercial name	Acid Red 114
Molecular formula	$C_{37}H_{28}N_4O_{10}S_3Na_2$
Purity	80%
Chromophore	Diazo
Molecular weight	830
Appearance	Dark red powder
Chemical name	Disodium 8-((3,3´-dimethyl-4´-(4-(4-methylphenylsulphonyloxy)phenylazo)(1,1´-biphenyl)-4-yl)azo)-7-hydroxynaphthalene-1,3-disulphonate

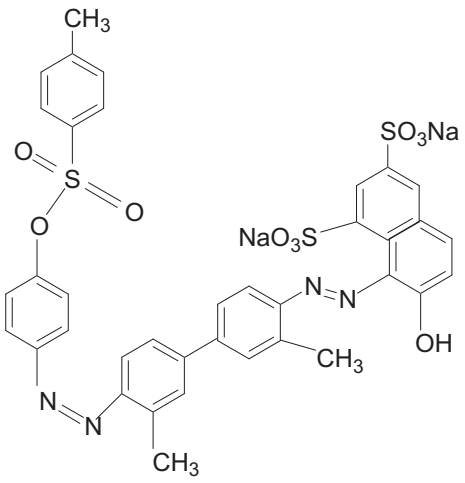

Fig. 1. Chemical structure of Acid Red 114.

2.2. Preparation of the adsorbent

The organobentonite was prepared by adding a quantity of the hexadecyltrimethylammonium ($HDTMA^+$) cations equal to two times the CEC of Na-bentonite. Twenty grams of Na-bentonite was added to 1,000 mL of HDTMA solution (284 mg/L) and stirred for 6 h at 60℃. The separated organobentonite was washed several times (about 10 times) with distilled water to remove the superficially held surfactant and filtered using Whatmann No. 42 filter paper. The product was dried at 70℃ for 24 h and was sieved between particle sizes 80 and 230 mesh (average particle size 0.096 mm).

2.3. Equipment and methods of characterization

X-ray powder diffraction measurements were performed on a Rigaku Geigerflex X-ray diffractometer with Ni-filtered Cu Kα radiation at 40 kV and 20 mA. The Fourier Transform Infrared (FTIR) spectra of the clay were recorded between 400 and 4,000 cm^{-1} using the KBr method with a NICOLET 400 D spectrophotometer. A Philips model XL 30 CP scanning electron microscope (SEM) was used to take micrographs of the clays. The thermogravimetric (TG) analyses were made on a Metler Toledo Star system under nitrogen atmosphere with a heating rate of 20℃ min^{-1}. The pH of zero point charge, pH_{zpc}, is defined as the pH of the suspension at which the surface charge density $\sigma_o = 0$. Potentiometric method [29] was used to measure the σ_o at different pH values. A Systronics pH meter model μ 362 (India) was employed to measure the potential and the pH of the solutions. The CEC of the clay samples was measured by $MgCl_2$ saturation and subsequent displacement by $CaCl_2$ [8]. Experiments were performed using a column operation method. One gram of the clay sample, which was previously saturated with $MgCl_2$, was weighed accurately and transferred into the column (10 × 0.4 cm). A sufficient quantity of distilled water was added to cover the adsorbent. A 100 mL separating funnel was filled with 0.1 M $CaCl_2$. This solution (100 mL) was allowed to drip into the column at a flow rate of 0.2 mL/min and the effluent was collected. The amount of Ca was estimated with atomic adsorption spectroscopy (AAS) after the entire solution passed through the column. The capacity of the adsorbent in milliequivalent per gram was calculated as the difference between the initial and final concentrations of Ca in the solutions.

2.4. Batch adsorption experiments

Batch experiments were conducted to determine the pH range at which the maximum adsorption of ions would take place. To a series of 100 mL flasks, each containing 0.1 g of the adsorbent, 50 mL of aqueous AR solution of the desired concentration were added. The initial pH was adjusted to values ranging from 2.0 to 9.0 using 0.1 mol/L NaOH and HCl. The suspension was shaken at 200 rpm for 6 h using a temperature-controlled flask shaker. The contents of the flask were centrifuged and the supernatants were analyzed for final pH and final AR concentrations. The concentration of AR remaining in the solutions was analyzed using a Schimadzu UV–Visible spectrophotometer at a wavelength of 514 nm. The amount of adsorption (q_e) was calculated by the following equation:

$$q_e = \frac{C_o - C_e}{m} V \quad (1)$$

where C_o and C_e were the initial and equilibrium AR concentrations, respectively. V and m were the volume of the solution and the amount of adsorbent used, respectively.

Kinetic experiments were carried out using 0.1 g of adsorbent and employing AR in the concentration range between 50 and 200 μmol/L in a temperature-controlled flask shaker. The samples were withdrawn at predetermined time intervals. The pH of the solution was adjusted to an optimum pH from the preliminary study by varying the pH between 2.0 and 9.0. Aliquots of the supernatants were withdrawn at different time intervals and the amount of AR in the solutions was estimated. Adsorption isotherm experiments were also performed by agitating 0.1 g of

adsorbent with 50 mL of the varying concentrations of AR at different temperatures (30–60℃). After the established contact time (6 h) was reached, aliquots of the supernatants were withdrawn and the amount of AR in the solutions was estimated. All the experiments were carried out in duplicate; the mean values are presented in this article.

2.5. Desorption and regeneration studies

To investigate the possibility of repeated adsorbent use, desorption and regeneration experiments were also conducted. The sorbate-loaded adsorbents were filtered and AR contents were measured. The spent adsorbent was added to a desorption medium (0.1 M NaOH) and the contents were shaken for 6 h, followed by centrifugation for separation. The desorbed AR was estimated. The sorbent thus regenerated was washed repeatedly with distilled water and used for further adsorption studies. The adsorption and desorption procedures were repeated for four cycles using the same adsorbent.

3. Results and discussion

3.1. Adsorbent characteristics

The FTIR spectra of Na-bentonite and organoclay are shown in Fig. 2. The adsorption bands around 3,625 cm^{-1} for Na-bentonite and 3,620 cm^{-1} organoclay may be due to the presence of adsorbed or hydration water as well as hydroxyl groups of octahedra such as Mg–OH–Al and Fe–OH–Al. [30]. The presence of adsorbed water is further confirmed by the presence of bands at 1,650 cm^{-1} (H–O–H bending) for organoclay and 1,645 cm^{-1} for Na-bentonite. A strong band observed for Na-bentonite at 1,050 cm^{-1} and at 1,025 cm^{-1} for organoclay is caused due to the vibration of Si–O or O–Si–O valence bonds. The additional peak at 1,425 cm^{-1} in organoclay, which is absent in Na-bentonite, indicates, the presence of C–N vibration in tertiary amine [22]. This observation clearly indicates that the surface modification of Na-bentonite was achieved by the surfactant.

SEM micrographs show (Fig. 3) the surface morphology of Na-bentonite and organoclay samples. It can be seen that Na-bentonite appears as corn flake-like crystals with a fluffy nature and curved plate-like structures. However, the clay treated with organic surfactant shows significant changes in its morphology. Compared with the morphology of Na-bentonite, there are many small and aggregated particles, and the

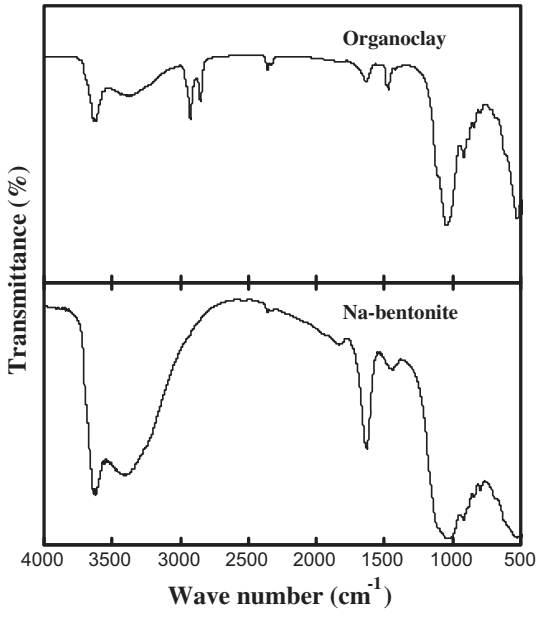

Fig. 2. The FTIR spectra of Na-bentonite and organo clay.

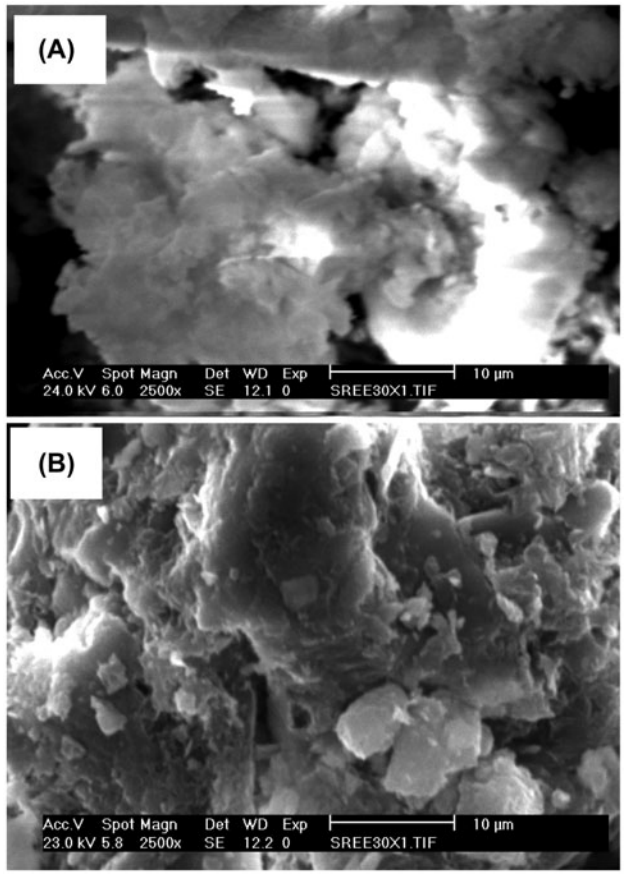

Fig. 3. SEM micrographs of Na-bentonite (A) and organoclay (B).

plates become relatively cloudy in the case of organoclay.

The XRD patterns of Na-bentonite and organoclay are shown in Fig. 4. The d-spacing at 4.56, 3.72, and 2.62 Å are characteristic of bentonite. The peak at 4.56 Å further confirmed the 2:1 mineral type. On treatment with surfactant, the basic structure of the aluminosilicate layer is maintained, while layer spacing was increased from 16.04 to 22.7 Å. The increase in basal spacing of Na-bentonite with $HDTMA^+$ cations could be attributed to replacement of the inorganic interlayer cations and their hydration water with $HDTMA^+$ cations.

The shape of perfectly straight chain $HDTMA^+$ cations looks like a "nail", and the chain end holding the three methyl group is the "nail head". When the $HDTMA^+$ cations lies stretched, the length of the "nail" is 25.3 Å, consisting of the "nail head" (4.3 Å) and "nail body" (21 Å). However, the height of the $HDTMA^+$ cations will vary with its orientation. When the plane of the zigzag arrangement of carbon atoms of $HDTMA^+$ cations is perpendicular to the plane of the Na-bentonite layer, the height of the "nail body" is ~4.6 Å and that of the "nail head" is 5.1 Å. However, the height of the "nail body" and "nail head" are 4.1 and 6.7 Å, respectively, when the plane of the zigzag arrangement of carbon atoms of $HDTMA^+$ cations is parallel to the plane of the Na-bentonite layer. Since the increase in d-spacing is only 6.6 Å after surfactant treatment, this value implies the lateral monolayer arrangement of $HDTMA^+$ cations within the interlayer space of Na-bentonite [31].

The TGA curves of the original Na-bentonite sample show losses of mass of about 14% up to a temperature of 200℃, which is caused by the dehydration of the interlayer cations (Fig. 5). Further losses of mass were found at 600℃. This feature is due to the expulsion of structural hydroxyls of the silicate layer. Organoclay shows an initial weight loss of 4.7% at 100℃, ending at 270℃ at which the weight loss was 8%. The lower weight loss for organoclay can be explained on the basis of comparatively stable binding of $HDTMA^+$ ions with Na-bentonite by the replacement of the inorganic interlayer cations of the clay. Furthermore, in organoclay, the $HDTMA^+$ cation samples are present at the surface and in the interlayer space. For $HDTMA^+$ cation samples present in the interlayer space, the thermal decomposition shifts to higher temperatures. Complete thermal decomposition of $HDTMA^+$ cations occur around 600℃.

The pH of zero point charge, pH_{ZPC}, is defined as the pH at which surface charge density (σ_o) is zero. The value of σ_o as a function of pH was calculated using the equation

$$\sigma_o = \frac{F(C_A - C_B + [OH^-] - [H^+])}{A} \quad (2)$$

where F is Faraday's constant, C_A and C_B are the concentrations of strong acid and strong base after each addition during titration. $[H^+]$ and $[OH^-]$, the equilibrium concentrations of H^+ and OH^- ions, respectively, are bound to the suspension surface. A is the surface area of the suspension. The plots of σ_o vs. pH for

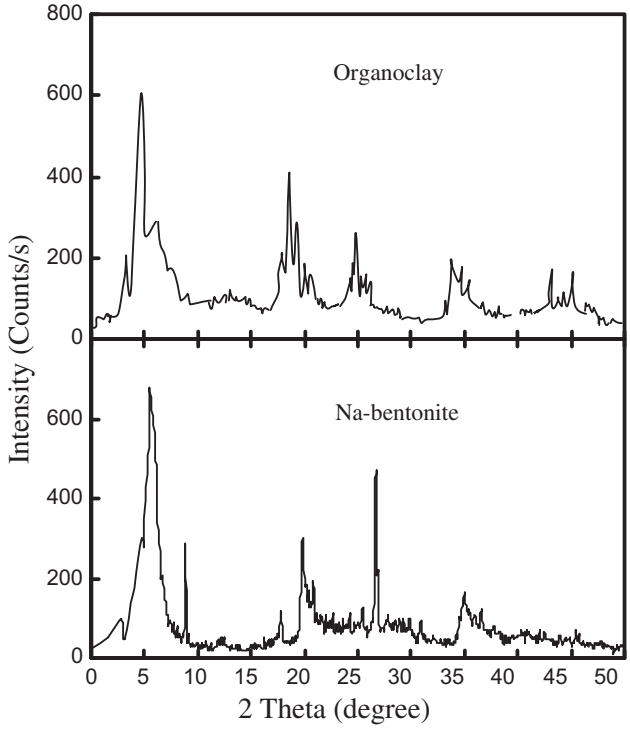

Fig. 4. X-ray diffraction patterns of Na-bentonite and organoclay.

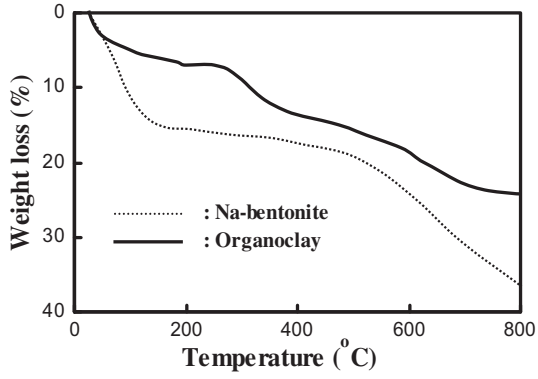

Fig. 5. TGA curves of Na-bentonite and Organoclay.

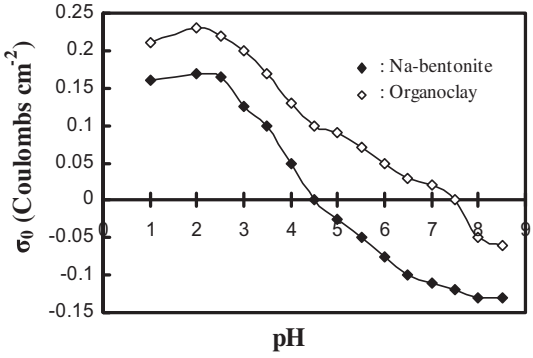

Fig. 6. Potentiometric titration curves depicting surface charge as function of solution pH.

Na-bentonite and organoclay are shown in Fig. 6. The point of intersection of σ_o with the pH curves gives the pH_{zpc} value of 4.2 and 7.6 for Na-bentonite and organoclay, respectively. The increase in pH_{zpc} after surfactant treatment indicates that organoclay becomes more positive and organophilic.

3.2. Effect of pH

The pH was the most important factor affecting the adsorption process. To study the influence of pH in the adsorption capacity of the prepared organoclay, experiments were performed using various initial pH values varying from 2.0 to 10.0 The variation in the adsorption of AR over a broad pH range of 2–10 is depicted in Fig. 7. It was seen that the lower the pH, the higher was the amount of AR adsorbed onto organoclay. Maximum percentage removal of AR was found to be at pH 3.0. Above and below this pH range, the extent of uptake was found to be considerably low. At an initial concentration of 100 and 200 μmol/L, AR removal shows 95.6% (47.8 μmol/g) and 82.2% (82.2 μmol/g), respectively. The removal efficiency of AR decreases with increase in pH. Surface charge of the organoclay is a function of pH. The pH at which the net charge of the organoclay becomes zero is referred to as zero point charge (pH_{zpc}). Below the pH_{zpc}, the surface has a net positive charge; above pH_{zpc}, the surface has a negative charge. Since the pH_{zpc} of organoclay was found to be 7.6, below this pH, a significantly high adsorption occurs between the positively charged clay surface and the negatively charged anionic dye. As the pH of the system increases, the number of negatively charged sites increases; negatively charged sites on the adsorbent do not favour the adsorption of anionic dyes due to the electrostatic repulsion [32]. In aqueous solution, the acid dye is first dissolved and sulfonate groups of the acid dye (D-SO_3Na) are dissociated and converted into anionic dye ion [1,33]. Also, the lower adsorption of AR at alkaline pH is due to the presence of excess hydroxyl ions competing with dye anions for the adsorption sites [11]. Similar results were also reported for the adsorption of Acid Red 114 onto activated carbon prepared from seed shell, which shows maximum adsorption at a pH of 3.0 [34].

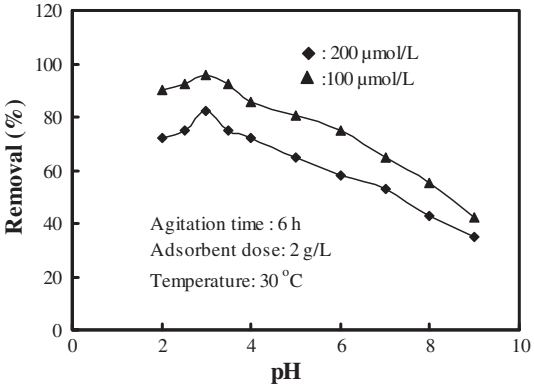

Fig. 7. Variation of percentage of adsorption of AR as a function of pH.

3.3. Effect of adsorbent dose on the removal of AR

The effect of adsorbent dose on the removal of AR by organoclay was investigated. Batch experiments were performed using 50 mL of 100 μmol/L of AR, adding different amount of Na-bentonite and organoclay (25–600 mg). For the complete removal of 100 μmol/L AR, it was observed that only 150 mg of organoclay was sufficient rather than 450 mg of Na-bentonite. This enhanced adsorptivity of organoclay may be due to the hydrophobic nature and porosity associated with organoclay when compared with Na-bentonite. The subsequent investigation on AR adsorption was only on organoclay.

3.4. Effect of contact time and initial concentration

The effect of contact time on the amount of AR adsorbed onto organoclay was investigated. When the contact time was increased, the amount of adsorption was also increased. The maximum adsorption capacity of AR onto organoclay was observed at 360 min, beyond which there was almost no further increase in the adsorption capacity, and it was thus fixed as the equilibrium contact time. For AR at an initial concentration of 100, 200, 400 and 600 μmol/L, the amount adsorbed at equilibrium was found to be 24.98

(99.9%), 48.2 (96.4%), 65.18 (86.9%) and 82.2 μmol/g (82.2%), respectively. The curves (figure not shown) were found to be single, smooth and continuous, leading to saturation, suggesting the possible monolayer coverage of AR on the surface of the adsorbent. With the lapse of time, AR showed increase in the amount adsorbed in both cases, but the percentage removal decreased with increase in concentration.

3.5. Adsorption kinetics

Several models could be used to express the mechanism of solute sorption onto a sorbent. In order to investigate the mechanism of sorption, characteristic constants of sorption were determined using a pseudofirst-order equation of Lagergren [35] based solid capacity. A linear form of pseudofirst-order model is

$$\log(q_e - q_t) = \log q_e - \frac{K_{ad}t}{2.303} \quad (3)$$

where q_t is amount of solute adsorbed at time t, q_e is amount adsorbed at equilibrium and K_{ad} is the Lagergren rate constant. The straight line plots of log ($q_e - q_t$) vs. time at different concentrations and at different temperatures for AR are shown in Fig. 8. The values

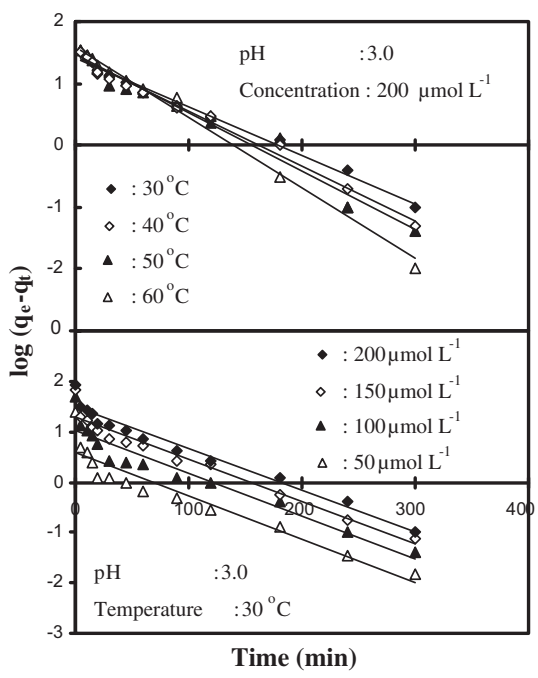

Fig. 8. Lagergren plots for the adsorption of AR onto organoclay at different concentrations and at different temperatures.

Table 2
Values of kinetic parameters for the adsorption of AR onto organo clay

Concentration (μmol L^{-1})	K_{ad} (min^{-1})	r^2
50	1.95×10^{-2}	0.977
100	1.95×10^{-2}	0.916
150	1.93×10^{-2}	0.950
200	1.81×10^{-2}	0.997
Concentration: 200 μmol/L		
Temperature (°C)	K_{ad} (min^{-1})	r^2
30	1.81×10^{-2}	0.988
40	2.04×10^{-2}	0.989
50	2.16×10^{-2}	0.975
60	2.60×10^{-2}	0.987

of K_{ad} at different initial concentrations (Table 2) clearly indicate that this parameter is totally independent of initial concentrations. The values of K_{ad} at different temperatures are also shown in Table 2. The increase in K_{ad} values with the increase in temperatures indicates the endothermic nature of the sorption process.

3.6. Adsorption isotherm

In order to determine the mechanism of AR adsorption onto organoclay and evaluate the relationship between adsorption temperatures, the experimental data were applied to the Langmuir and Freundlich isotherm equations. The constant parameters of the isotherm equations for this adsorption process were calculated by regression using the linear form of the isotherm equations. The constant parameters and correlation coefficient (r^2) are summarized in Table 3.

Langmuir proposed a theory to describe the adsorption of gas molecules onto metal surfaces. The Langmuir adsorption isotherm has been successfully applied to many real sorption processes. The linearized Langmuir isotherm is represented by following equation:

$$\frac{C_e}{q_e} = \frac{1}{Q^\circ b} + \frac{C_e}{Q^\circ} \quad (4)$$

where C_e is the solute concentration at equilibrium (μmol/L), q_e the adsorption capacity at equilibrium (μmol/g), b is the Langmuir adsorption constant (L/μmol) and Q° is the monolayer adsorption capacity.

At pH 3.0, the values of Q° were found to be 140.84, 196.07, 222.2 and 256.4 μmol/g at 30, 40, 50, 60°C, respectively, for AR. The values of Q° increase

Table 3
Langmuir and Freundlich constants for the adsorption of AR onto organoclay

	Langmuir constants			Freundlich constants		
Temperature (℃)	Q° (μmol/g)	b (L/μmol)	r^2	K_F	$1/n$	r^2
30	140.84	0.073	0.989	42.49	0.209	0.977
40	196.07	0.083	0.981	34.60	0.304	0.992
50	222.22	0.091	0.986	72.50	0.205	0.978
60	256.40	0.102	0.999	109.5	0.139	0.901

with rise in temperature, thereby confirming that the process is endothermic [36,37].

As the initial concentration varies from 50 to 500 μmol/L, the amount of AR adsorption increased from 24.97 to 137.35 μmol/g at 30℃ and from 48.66 to 181.87 at 40℃, respectively. The amount of adsorption increases from 49.95 to 219.01 μmol/g at 50℃ as the initial concentration increased from 100 to 600 μmol/L. As the initial concentration increased from 200 to 800 μmol/L, the amount of adsorption increased from 99.91 to 248.01 μmol/g at 60℃.

The Freundlich adsorption isotherm can be expressed as

$$\ln q_e = \ln K_F + \frac{1}{n} \ln C_e \quad (5)$$

where K_F and $1/n$ are isotherm constants which indicate the capacity and intensity of adsorption, respectively. Table 3 indicates Freundlich adsorption isotherm constants along with their correlation coefficients.

The values of K_F and n determined from the Freundlich isotherm model change with the rise in temperature. The values of n for the Freundlich isotherm were found to be greater than 1, indicating that AR was favourably adsorbed by organoclay at all temperatures studied [8,38]. The values of n were found to be 4.78, 3.29, 4.86 and 7.20 at 30, 40, 50 and 60℃, respectively, for AR.

The validity of the isotherm models were tested by comparing the experimental and calculated data (Fig. 9). Based on the correlation coefficient (r^2), it was noted that the Langmuir equation gave a best fit over the entire range of concentrations. The essential characteristic of the Langmuir isotherm can be described by a separation factor R_L, which is defined by $R_L = 1/(1 + b\ C_o)$. The values of R_L between 0 and 1 at different concentrations and temperatures indicate favourable adsorption of AR onto organoclay.

The literature contains few studies of the adsorption of AR on soy meal hull (Q° = 109.89 μ mol g^{-1}) [9] and

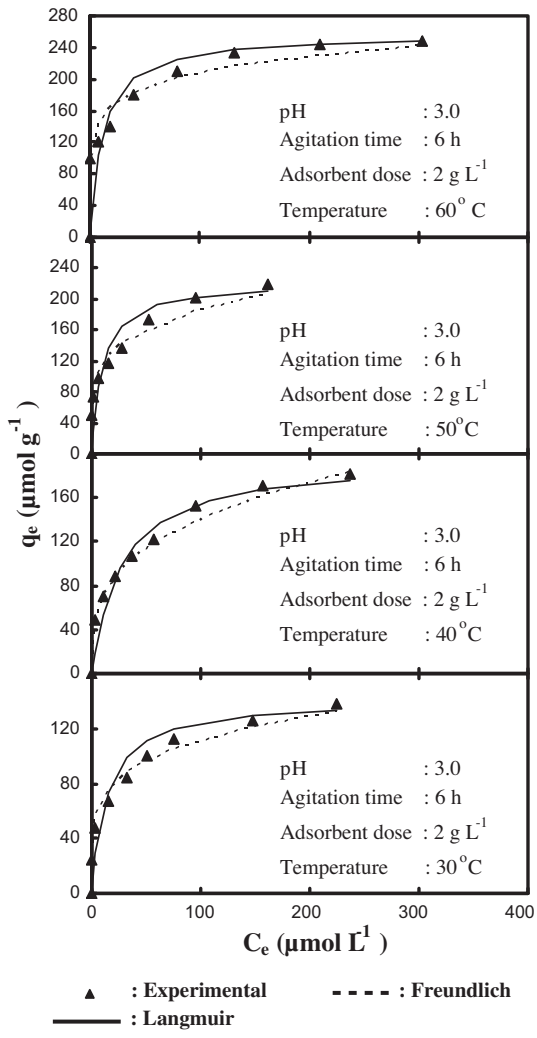

Fig. 9. Comparison of the experimental and model fits of the Langmuir and Freundlich isotherms for the adsorption of AR onto organoclay.

Acid Red 57 onto calcined alunite (Q° = 140 μmol/g) [11]. These adsorption capacity results show that organoclay is a good adsorbent for the removal of AR (Q° = 140.08 μmol/g) from aqueous solutions when

Table 4
Thermodynamic parameters for the adsorption of AR onto organoclay

Temperature (°C)	b (L/mol)	ΔG° (kJ/mol)	ΔH° (kJ/mol)	ΔS° (J/K/mol)
30	73×10^3	−28.18	9.22	123.53
40	83×10^3	−29.45		
50	91×10^3	−30.64		
60	102×10^3	−31.92		

compared with soy meal hull, whereas the value of monolayer capacity shown by calcined alunite is comparable with organoclay. The estimated cost of the adsorbent organoclay, after consideration of the expenses for bentonite, HDTMA, NaCl, electrical energy, supplies and labor would be approximately US $ 50 per kg.

The thermodynamic parameters such as free energy change (ΔG°), enthalpy change (ΔH°) and entropy change (ΔS°) for the adsorption process were calculated using the equations

$$\Delta G^\circ = -RT \ln b \tag{6}$$

$$\ln b = \frac{\Delta S^\circ}{R} - \frac{\Delta H^\circ}{RT} \tag{7}$$

The plot of lnb vs. $1/T$ (figure not shown) was found to be linear. The values of ΔH° and ΔS° were obtained from the slope and intercept of the plot. The positive value of ΔH° indicates that AR (9.22 kJ/mol) adsorption onto organoclay is endothermic. The negative values of ΔG° for solute removal indicate the spontaneous nature of adsorption. The positive value of ΔS° indicates the higher order of reaction (123.53 J/K/mol) during the adsorption of AR onto organoclay and also reflects the affinity of adsorbent materials for the solute particles. The values of thermodynamic parameters for the adsorption of AR were presented in Table 4.

3.7. Desorption and regeneration studies

To make the adsorption process more economical, it is necessary to regenerate the spent adsorbent. Desorption studies of the adsorbed AR from spent adsorbent was studied. The organoclay loaded with maximum amount of sorbate was tested using 0.1 M NaOH solution. The results of the multiple adsorption/desorption cyclic test to investigate the suitability of the organoclay are presented in Table 5. An efficiency of 92.2% desorption for AR was obtained using 0.1 M NaOH and was therefore suitable for the regeneration of sorbate from spent organoclay. The recovery percentage reduced to 88.7 and 87.3% for AR at the end of fourth cycle. The small fraction of adsorbed solute not recoverable by regeneration, presumably represent the species, which was bound through strong interaction, and, as a result, sorption capacity is reduced in successive cycles.

Table 5
Four cycles of AR adsorption–desorption with 0.1 M NaOH as the desorbing agent

	Adsorption		Desorption	
	μmol/g	%	μmol/g	%
1	24.98	99.9	23.05	92.2
2	24.15	96.6	21.52	89.1
3	23.42	93.7	20.51	87.5
4	22.38	89.5	19.56	87.3

Note: (Adsorbent dose = 2 g/L; pH 3.0; Equilibrium time = 6 h; Temperature = 30 °C; Initial concentration = 50 μmol/L).

4. Conclusions

Recently, adsorption due to clay has drawn much attention due to its low cost, easy availability and the possibility of enhanced adsorbabilities by surface modification. The performance of HDTMA-intercalated bentonite clay (oganoclay) for the removal of AR from aqueous solutions has been evaluated in this study. The surface and physical properties of Na-bentonite and organoclay were compared using SEM, XRD, IR, thermal analysis etc. The point of intersection of σ_o with the pH curves gives the pH_{zpc} value of 7.6 and 4.2 for organoclay and Na-bentonite, respectively. The increase in pH_{zpc} after surfactant treatment indicates that organoclay becomes more positive and organophilic.

Adsorption of AR onto organoclay was studied and was found to be pH dependent. It is seen that the lower the pH, the higher was the amount of AR adsorbed onto organoclay. Maximum percentage removal of AR was found to be at pH 3.0. The effect of adsorbent dose on the removal of AR by organoclay was investigated. It was observed that for the

complete removal of 100 μmol L^{-1}, only 150 mg of organoclay was sufficient, rather than 450 mg of Na-bentonite. The experimental data were applied to the Langmuir and Freundlich isotherm equations. At pH 3.0, the values of Q° were found to 140.84, 196.07, 222.2 and 256.4 μmol g^{-1} for AR at 30, 40, 50 and 60˚C, respectively. The values of Q° increase with rise in temperature, thereby confirming that the process is endothermic. The Freundlich isotherm model was also used to study the isotherm. However, based on the correlation coefficient (r^2), it was found that the Langmuir equation gave the best fit over the entire range of concentrations.

In order to investigate the mechanism of sorption, characteristic constants of sorption were determined using a pseudo-first order equation of Lagergren-based solid capacity. Desorption of the adsorbed AR from the spent adsorbent were also studied using 0.1 M NaOH solution, and it was found that almost 92.2% desorption for AR was obtained using 0.1 M NaOH, and is therefore suitable for regeneration of sorbate from spent organoclay.

Acknowledgements

The authors are thankful to the Professor and Head, Department of Chemistry, University of Kerala, for providing laboratory facilities.

References

[1] Y.C. Wong, Y.S. Szeto, W.H. Cheung, G. McKay, Adsorption of acid dyes on chitosan—equilibrium isotherm analyses, Process Biochem. 39 (2004) 695–704.
[2] T. Robinson, B. Chandran, P. Nigam, Removal of dyes from a synthetic textile dye effluent by biosorption on apple pomace and wheat straw, Water Res. 36 (2002) 2824–2830.
[3] D. Mohan, K.P. Singh, G. Singh, K. Kumar, Removal of dyes from wastewater using flyash, a low-cost adsorbent, Ind. Eng. Chem. Res. 41 (2002) 3688–3695.
[4] P. Nigam, G. Armour, I.M. Banat, D. Singh, R. Marchant, Physical removal of textile dyes from effluents and solid-state fermentation of dye-adsorbed agricultural residues, Bioresour. Technol. 72 (2000) 219–226.
[5] K.R. Ramakrishna, T. Viraraghavan, Dye removal using low cost adsorbents, Water Sci. Technol. 36 (1997) 189–196.
[6] V.K. Garg, R. Kumar, R. Gupta, Removal of malachite green dye from aqueous solution by adsorption using agro-industry waste: A case study of *Prosopis cineraria*, Dyes Pigm. 62 (2004) 1–10.
[7] R. Sanghi, B. Bhattacharya, Review on decolorisation of aqueous dye solutions by low cost adsorbents, Coloration Technol. 118 (2002) 256–269.
[8] P.K. Malik, Use of activated carbons prepared from sawdust and rice-husk for adsorption of acid dyes: A case study of Acid Yellow 36, Dyes Pigm. 56 (2003) 239–249.
[9] M. Arami, N.Y. Limaee, N.M. Mahmoodi, N.S. Tabrizi, Equilibrium and kinetics studies for the adsorption of direct and acid dyes from aqueous solution by soy meal hull, J. Hazard. Mater. 135 (2006) 171–179.
[10] E.J. Weber, N. Lee Wolfe, Kinetic studies of the reduction of aromatic AZO compounds in anaerobic sediment/water systems, Environ. Toxicol. Chem. 6 (1987) 911–919.
[11] S. Tunali, A.S. Ozcan, A. Ozcan, T. Gedikbey, Kinetics and equilibrium studies for the adsorption of Acid Red 57 from aqueous solutions onto calcined-alunite, J. Hazard. Mater. 135 (2006) 141–148.
[12] V. Meshko, L. Markovska, M. Mincheva, A.E. Rodrigues, Adsorption of basic dyes on granular acivated carbon and natural zeolite, Water Res. 35 (2001) 3357–3366.
[13] N. Kannan, M.M. Sundaram, Kinetics and mechanism of removal of methylene blue by adsorption on various carbons—A comparative study, Dyes Pigm. 51 (2001) 25–40.
[14] G. Annadurai, R.S. Juang, D. Lee, Use of cellulose-based wastes for adsorption of dyes from aqueous solutions, J. Hazard. Mater. B 92 (2002) 263–274.
[15] R.A. Shawabkeh, M.F. Tutunji, Experimental study and modeling of basic dye sorption by diatomaceous clay, Appl. Clay Sci. 24 (2003) 111–120.
[16] M. Dogan, M. Alkan, A. Türkyilmaz, Y. Ozdemir, Kinetics and mechanism of removal of methylene blue by adsorption onto perlite, J. Hazard. Mater. B109 (2004) 141–148.
[17] B. Acemioglu, Batch kinetic study of sorption of methylene blue by perlite, Chem. Eng. J. 106 (2004) 73–81.
[18] T.A. Sibel, U. Recep, Untreated clay with high adsorption capacity for effective removal of C.I. Acid Red 88 from aqueous solutions: Batch and dynamic flow mode studies, Chem. Eng. J. 162 (2010) 591–598.
[19] X. Duanping, G. Changjian, C. Xiao, Adsorption and removal of Acid red 3R from Aqueous Solution Using Flocculent Humic Acid isolated from Lignite, Procedia Environ. Sci. 18 (2013) 127–134.
[20] S. Ran-ran, Y. Liang-guo, Y. Kun, Y. Shu-jun, H. Yuan-feng, Y. Hai-qin, D. Bin, Magnetic Fe_3O_4/MgAl-LDH composite for effective removal of three red dyes from aqueous solution, Chem. Eng. J. 252 (2014) 38–46.
[21] T. Polubesova, G. Rytwo, S. Nir, C. Serban, L. Margulies, Adsorption of benzyltrimethylammonium and benzyltriethylammonium on montmorillonite: Experimental studies and model calculations, Clays Clay Miner. 45 (1997) 834–841.
[22] T.S. Anirudhan, M. Ramachandran, Adsorptive removal of tannin from aqueous solutions by cationic surfactant-modified bentonite clay, J. Colloid Interface. Sci. 299 (2006) 116–124.
[23] T. Kwolek, M. Hodorowicz, K. Stadnicka, J. Czapkiewicz, Adsorption isotherms of homologous alkyldimethylbenzylammonium bromides on sodium montmorillonite, J. Colloid Interface. Sci. 264 (2003) 14–19.

[24] S.K. Dentel, J.Y. Bottero, K. Khatib, H. Demougeot, J.P. Duguet, C. Anselme, Sorption of tannic acid, phenol, and 2,4,5-trichlorophenol on organoclays, Water Res. 29 (1995) 1273–1280.
[25] S.M. Koh, J.B. Dixon, Preparation and application of organo-minerals as sorbents of phenol, benzene and toluene, Appl. Clay Sci. 18 (2001) 111–122.
[26] S. Yun-Hwei, Removal of phenol from water by adsorption–flocculation using organobentonite, Water Res. 36 (2002) 1107–1114.
[27] T.S. Anirudhan, M. Ramachandran, Removal of 2,4,6-trichlorophenol from water and petroleum refinery industry effluents by surfactant-modified bentonite, J. Water Process Eng. 1 (2014) 46–53.
[28] F. Rasouli, S. Aber, D. Salari, A.R. Khataee, Optimized removal of Reactive Navy Blue SP-BR by organo-montmorillonite based adsorbents through central composite design, Appl. Clay Sci. 87 (2014) 228–234.
[29] J.A. Schwarz, C.T. Driscoll, A.K. Bhanot, The zero point of charge of silica–alumina oxide suspensions, J. Colloid Interface Sci. 97 (1984) 55–61.
[30] D.S. Orlov, Soil Chemistry, Oxford/IBH, New Delhi, 1992.
[31] H. Hongping, L.F. Ray, B. Thor, Y. Peng, D. Loc, Y. Dan, X. Yunfei, J.T. Kloprogge, Changes in the morphology of organoclays with $HDTMA^+$ surfactant loading, Appl. Clay Sci. 31 (2006) 262–271.
[32] C. Namasivayam, D. Kavitha, Removal of Congo Red from water by adsorption onto activated carbon prepared from coir pith, an agricultural solid waste, Dyes Pigm. 54 (2004) 47–58.
[33] I.D. Mall, V.C. Srivastava, N.K. Agarwal, I.M. Mishra, Removal of Congo Red from aqueous solution by bagasse fly ash and activated carbon: Kinetic study and equilibrium isotherm analyses, Chemosphere 61 (2005) 492–501.
[34] N. Thinakaran, P. Panneerselvam, P. Baskaralingam, D. Elango, S. Sivanesan, Equilibrium and kinetic studies on the removal of Acid Red 114 from aqueous solutions using activated carbons prepared from seed shells, J. Hazard. Mater. 158 (2008) 142–150.
[35] S. Lagergren, B.K. Sevenska Handl, 1898, as sited by G.N. Manju, C. Raji, T.S. Anirudhan, Evaluation of coconut husk carbon for the removal of arsenic from water, Water Res. 32 (1998) 3062–3070.
[36] M. Ajmal, R.A.K. Rao, R. Ahmad, J. Ahmad, Adsorption studies on *Citrus reticulata* (fruit peel of orange): removal and recovery of Ni(II) from electroplating wastewater, J. Hazard. Mater. B 79 (2000) 117–131.
[37] V.K. Gupta, A. Mittal, V. Gajbe, Adsorption and desorption studies of a water soluble dye, Quinoline Yellow, using waste materials, Colloid Interface Sci. 284 (2005) 89–98.
[38] Canan Akmil Başar, Applicability of the various adsorption models of three dyes adsorption onto activated carbon prepared waste apricot, J. Hazard. Mater. B 135 (2006) 232–241.